A VOLTAGE-CONTROLLED VARACTORLESS LC-TANK OSCILLATOR WITH A TRANSFORMER-FEEDBACK TECHNIQUE

Ching-Yuan Yang and Meng-Ting Tsai
Department of Electrical Engineering, National Chung Hsing University, 250 Kuo-Kuang Road, Taichung, Taiwan 40254;
Corresponding author: ycy@dragon.nchu.edu.tw

ABSTRACT: *A differential-voltage-controlled LC oscillator employs a g_m-tuned technique instead of a varactor is presented, verified, and measured. The design was demonstrated in a standard 0.18-μm CMOS process. The oscillator can operate at the range of 4.73–5.05 GHz under a 1.8-V supply voltage. The measured phase noise is −100.76 dBc/Hz at 100-kHz frequency offset and −121.53 dBc/Hz at 1-MHz frequency offset away from the 4.73-GHz carrier with power consumption of 6.48 mW.* © 2007 Wiley Periodicals, Inc. Microwave Opt Technol Lett 49: 2808–2810, 2007; Published online in Wiley InterScience (www.interscience.wiley.com). DOI 10.1002/mop.22861

1. INTRODUCTION

Recently, interest in LC-based voltage-controlled oscillators (VCOs) has surged with the growing demand for radio frequency communication systems. Although some types of oscillators such as relaxation oscillators, ring oscillators, etc., implemented in advanced submicron CMOS technology may also be capable of achieving gigahertz operation frequencies, nowadays, their phase noise behavior and frequency stability at high frequencies are still not good enough for communication applications. *LC*-tank oscillators are the only type of integrated oscillators that will be capable of achieving the required high frequencies and low noise at reasonable power consumption. Unlike a conventional *LC* VCO using a varactor to tune oscillating frequencies, we propose a varactorless VCO employing a tunable transconductance for frequency control.

2. VARACTORLESS VCO IMPLEMENTATION

2.1. Proposed Varactorless VCO

To replace the varactor, the *LC*-VCO scheme with a tunable g_m-based technique is shown in Figure 1. The VCO circuit is
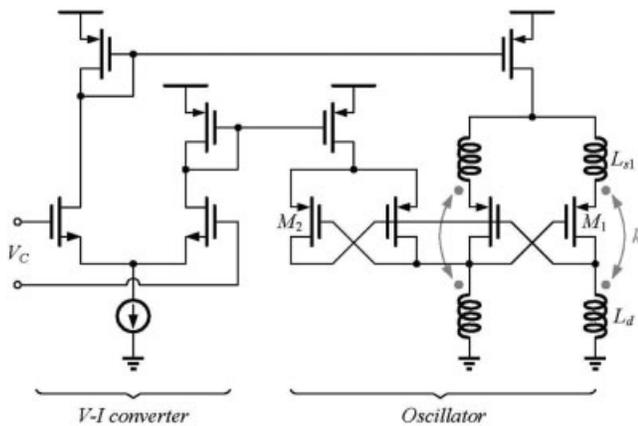
Figure 1 Varactorless VCO
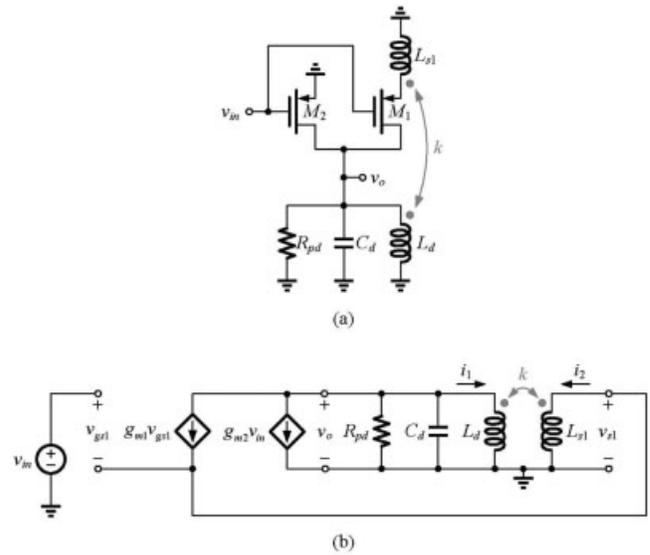
Figure 2 (a) Half-circuit equivalent of Figure 1 and (b) small-signal equivalent circuit

divided into two parts: one is the *LC* oscillation scheme and the other is the *V-to-I* converter. The *V-to-I* converter is a simplified differential pair circuit and is used to produce the bias current for tuning g_m that exhibits in the oscillator. The *LC* oscillator generates the operation frequency, formed by two PMOS differential pairs in cross-connection with and without transformer feedback, respectively [1]. Besides the effective values of the inductor and capacitor in the tank, the oscillation frequency depends upon g_m of the PMOS transistors.

2.2. Simplified Linear Analysis of the Proposed VCO

Suggesting only the inductor value can be active on the source of the transistor M_1, a half-circuit concept is shown in Figure 2(a), where R_{pd} and C_d represent the equivalent parallel resistance and capacitance in the primary coil where the oscillation occurs. With the small-signal equivalent circuit depicted in Figure 2(b), we can obtain the transfer function

$$\frac{v_o}{v_{in}}(s) = -\frac{s^2 g_{m1}g_{m2}\Delta + s(g_{m1}L_d + g_{m2}L_d - g_{m1}M)}{s^3 g_{m1}\Delta C_d + s^2\left(L_d C_d + \frac{g_{m1}\Delta}{R_{pd}}\right) + s\Gamma + 1}, \quad (1)$$

where $\Delta = L_d L_{s1} - M^2$ and $\Gamma = \frac{L_d}{R_{pd}} + g_{m1}(L_{s1} - M)$. Since the oscillator can be viewed as two stages of Figure 2(a) in a cascade, the gain around the loop is given by

$$G(j\omega) = \left(\frac{v_o}{v_{in}}(j\omega)\right)^2. \quad (2)$$

At resonance, the total phase shift around the loop is zero because each stage contributes zero frequency-dependent phase shifts. The loop gain will be a real number (i.e., the phase will be zero) at the oscillation frequency ω_0, given by

$$\omega_0^2 = \frac{\Lambda + \sqrt{\Lambda^2 + 4g_{m1}^2 g_{m2}(g_{m1}L_d + g_{m2}L_d - g_{m1}M)\Delta^2 C_d}}{2g_{m1}^2 g_{m2}\Delta^2 C_d},$$

$$\quad (3)$$

where $\Lambda = g_{m1}^2[g_{m2}(L_{s1} - M) - (L_d - M)/R_{pd}]\Delta - (g_{m1}L_d + g_{m2}L_d - g_{m1}M)L_dC_d$. The oscillation frequency obviously depends on the inductances and capacitances of the tank as well as the transconductances, g_{m1} and g_{m2}. To understand the tuning range of the VCO, two extremes of the control voltage can be discussed.

1. At one extreme of the control voltage, only the differential pair of M_2's is active and the one of M_1's is disabled, yielding the maximum oscillation frequency. With $g_{m1} = 0$, we have

$$\frac{v_o}{v_{in}}(s) = -\frac{sg_{m2}L_d}{s^2L_dC_d + s\dfrac{L_d}{R_{pd}} + 1}. \tag{4}$$

It can be easy to see that the oscillation frequency is

$$\omega_1 = \frac{1}{\sqrt{L_dC_d}}, \tag{5}$$

and the quality factor is defined as

$$Q_0 = R_{pd}\sqrt{\frac{C_d}{L_d}}. \tag{6}$$

2. Conversely, at the other extreme, only the differential pair of $M1$'s is on and the one of $M2$'s is off, providing the minimum oscillation frequency. For $gm2 = 0$, substituting $s = j\omega$ results in

$$\frac{v_o}{v_{in}}(j\omega) =$$

$$-\frac{j\omega g_{m1}(L_d - M)}{1 - \omega^2\left(L_dC_d + \dfrac{g_{m1}\Delta}{R_{pd}}\right) + j\omega(\Gamma - \omega^2 g_{m1}\Delta C_d)}. \tag{7}$$

Applying the imaginary part of the denominator to zero, we obtain the oscillation frequency as

$$\omega_2 = \frac{1}{\sqrt{L_dC_d + \dfrac{g_{m1}\Delta}{R_{pd}}}}. \tag{8}$$

Next, we will develop a simple quality factor analysis to verify the performance of the VCO. For an ideal coupling factor $k = 1$, Δ approximates to zero and we have

$$\frac{v_o}{v_{in}}(s) \approx -\frac{s(g_{m1}L_d + g_{m2}L_d - g_{m1}M)}{s^2L_dC_d + s\Gamma + 1}. \tag{9}$$

An important parameter is the loaded quality factor Q_{LD} of the tank circuit, which is defined as the Q factor of the second-order transfer function v_o/v_{in}. From Eq. (9), the load quality factor is given by

$$Q_{LD} = \frac{\sqrt{L_dC_d}}{\dfrac{L_d}{R_{pd}} + g_{m1}(L_{s1} - M)}. \tag{10}$$

Although Eq. (10) provides essential insights into the Q, how to implement an electrical oscillator is a more practical design work. Two important concepts of low noise performance and tuning range in the design regime have to be considered. Assuming $L_{s1} > M$, the denominator is larger than L_d/R_{pd}, resulting in that the load quality factor becomes lower compared with that in Eq. (4). Selecting $L_{s1} < M$, therefore, the load quality increases and becomes larger than Q_0 in conventional schemes. Besides, the oscillation frequency lowers as g_{m1} increases. As a result, maximizing the value of g_{m1} can directly increase both the tuning rang and the quality factor.

2.3. Transformer Realization

Depicted in Figure 3 is a monolithic transformer realized by inter-winding two spiral inductors. Octagonal spiral geometry is adopted because a spiral structure that more closely approximates a circle is preferred to increase the quality factor. The primary coil L_d in the resonator is mainly made of the top metal layer, i.e., Metal 6 layer, which is furthest from the conductive substrate and is the thickest metal layer, while Metal 4 layer is used to form the secondary coil. The primary is designed in two turns, 9-μm width, 2-μm line spacing, and an outer radius of 60 μm, and the secondary coil has the same width and outer radius but one turn structure. They are modeled as a combination of two separate π models for the transformer [2, 3]. With the mutual magnetic and capacitive coupling, the simulated inductor values are: $L_d = 0.59$ nH and $L_{s1} = 0.26$ nH, and the coupling coefficient k is 0.7. The quality factor is around nine at the oscillation frequency.

3. EXPERIMENTAL RESULTS

To verify performance of the proposed VCO, as previously described, the proposed circuit was fabricated in 0.18-μm CMOS technology. Figure 4 shows the microphotograph of the test chip. The core circuit occupies an active area of 840×690 μm^2 including the output buffers and I/O pads. Each output signal is connected to an open-drain circuit with an externally match resistance of 50 Ω. The VCO was tested on an FR-4 PC board using Agilent E4407B Spectrum Analyzer for measurement. The VCO consumes the current of 3.6 mA under a 1.8-V supply voltage. The measured output power is around -3 dBm. Figure 4 shows both the simulated and measured frequency-tuning characteristics. As can be seen, the measured tuning range is 6% (4.73–5.05 GHz). Figure 5 also shows the plots of the simulated and measured phase noise at 1-MHz offset from the carrier for the control voltage. The measured values of phase noise are from -113 dBc/Hz to -122 dBc/Hz at 1-MHz offset. The minimum phase noise of the VCO occurs at minimum operating frequencies. Figure 6 shows the phase noise at 4.73 GHz and the measured noise is -101 dBc/Hz at 100-kHz offset, -122 dBc/Hz at 1-MHz offset, and -142 dBc/Hz at 10-MHz offset.

Using a linear theory [4], an oscillator's phase-noise model is given by
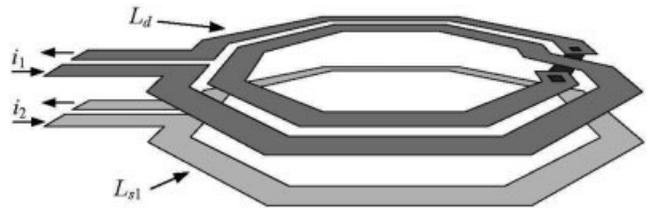
Figure 3 Transformer realization
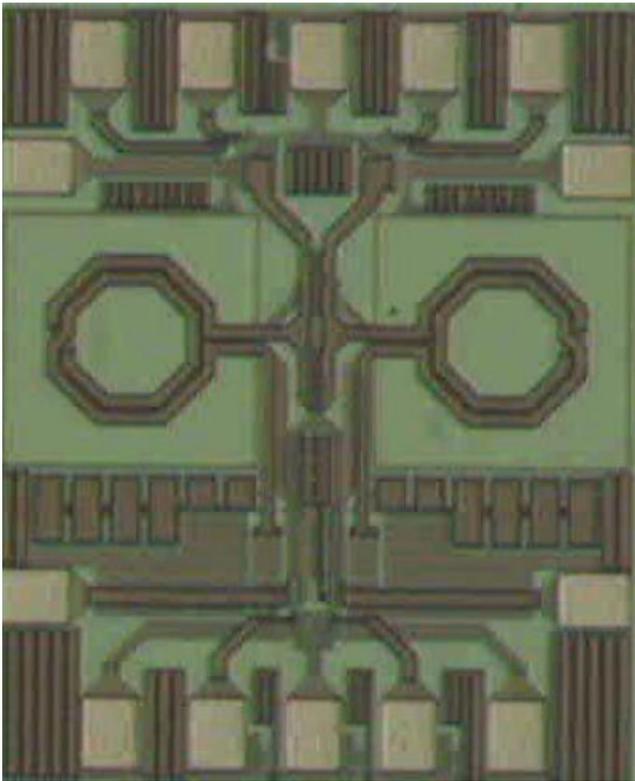
Figure 4 Die photo of the fabricated VCO chip. [Color figure can be viewed in the online issue, which is available at www.interscience.wiley.com]

$$L(\Delta\omega) = 10 \log\left[\frac{2FkT}{P_{\text{sig}}}\left(1 + \frac{\omega_0}{2Q_{\text{tank}}\Delta\omega}\right)\right], \qquad (11)$$

where ω_0 is the center frequency, $\Delta\omega$ is the frequency offset, Q_{tank} is the tank quality factor, F is the excess noise factor, P_{sig} is the oscillation signal power, and $L(\Delta\omega)$ is the phase noise measured at $\Delta\omega$. The phase noise performance is mainly due to the characteristics of the tank circuit. From Eq. (10), increasing g_{m1} increases the quality factor and thereby lowers the phase noise. As observed in Figure 5, the phase noise is decreased as the control voltage increases to drive larger g_{m1}.

4. CONCLUSION

It is an interesting work covering the use of a g_{m}-tuned technique in place of tunable capacitors (e.g., varactors) for building high-
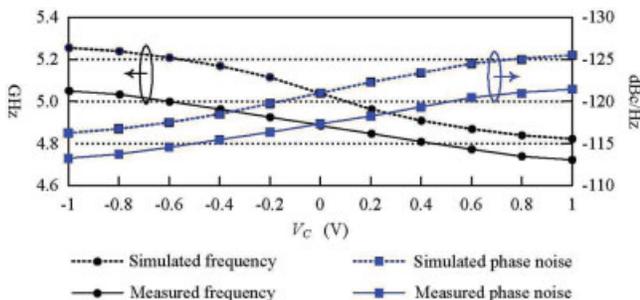
Figure 5 Simulated and measured characteristics of tuning frequency range and phase noise value at 1-MHz offset. [Color figure can be viewed in the online issue, which is available at www.interscience.wiley.com]
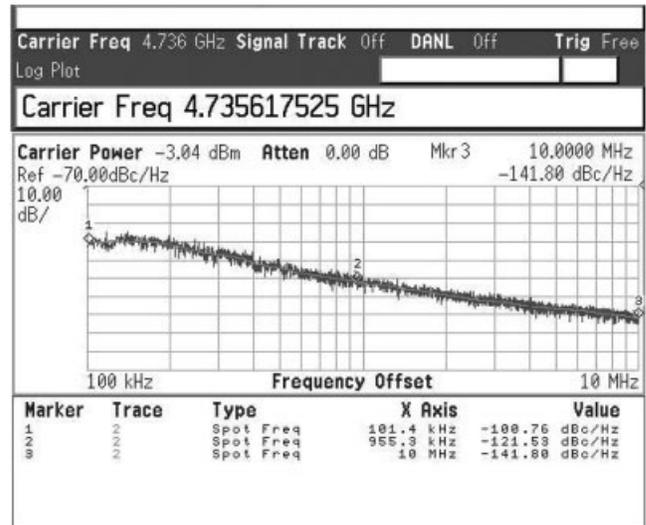
Figure 6 Measured phase noise of the VCO at 4.73 GHz

frequency VCOs. The prototype *LC*-VCO utilizes the g_{m}-tuned technique to extend the operating frequencies at 4.73–5.05 GHz in a standard 0.18-μm CMOS process at the operating supply voltage of 1.8 V. The measured results demonstrate the functionality of the *LC* VCOs with the g_{m}-tuned technique.

REFERENCES

1. K. Kwok and H.C. Luong, Ultra-low-voltage high-performance CMOS VCOs using transformer feedback, IEEE J Solid State Circ 40 (2005), 652–660.
2. Taiwan Semiconductor Manufacturing Co., Ltd, TSMC 0.18-μm Mixed Signal 1P6M Salicde 1.8V/3.3V RF Spice Models, Ver. 1.3. (2004).
3. J.R. Long, Monolithic transformers for silicon RF IC design, IEEE J Solid State Circ 35 (2000), 1368–1382.
4. D.B. Leeson, A simple model of feedback oscillator noise spectrum, Proc IEEE 54 (1966), 329–330.

NONRECIPROCAL LEFT HANDED COPLANAR WAVEGUIDE OVER FERRITE SUBSTRATE WITH ONLY SHUNT INDUCTIVE LOAD

Mahmoud A. Abdalla and Zhirun Hu
Microwave and Communications Systems Group, School of Electrical and Electronic Engineering, University of Manchester, P.O Box 88, Manchester M60 1QD, United Kingdom; Corresponding author: mody_m_1981@yahoo.com

ABSTRACT: *A novel ferrite nonreciprocal left-handed (LH) transmission line is presented. The proposed structure is composed of a co-*